2

Wind Modelling and its Possible Application to Control of Wind Farms

Yoshito Hirata, Hideyuki Suzuki, and Kazuyuki Aihara

Because of global warming and oil depletion, the number of wind turbines is increasing. Wind turbines commonly have a horizontal axis, but some wind turbines have a vertical axis. A problem of wind turbines with horizontal axis is that we need to face them towards the wind for maximising energy production. If the geography around a wind turbine is complicated, then the wind direction keeps changing. Thus, if one can predict the wind direction to some extent, then one may generate more electricity by controlling wind turbines according to the prediction.

In this chapter, we discuss how to model the wind. First, we formulate a problem and clarify which properties of the wind we need to predict. Second, we discuss the characteristics for time series of the wind. Third, we model the wind based on the knowledge and predict it. We prepare different models for predicting wind direction and absolute wind speed. Finally, we apply the prediction and simulate control of a wind turbine. Since we integrate predictions for wind direction and absolute wind speed to obtain an optimal control, the whole scheme can be regarded as heterogeneous fusion.

2.1 Formulating Yaw Control for a Wind Turbine

There are three purposes for predicting the wind in applications of wind turbine. The first purpose is to estimate energy production by wind turbines in the future. By estimating the energy production, we can prepare other sources of energy production to meet the demand. The time scale of the prediction for this purpose ranges from 30 min to some days and the prediction can be done by either a medium-range weather forecasts [20] or time series prediction [2–4]. The second purpose is to avoid gusts. For this purpose, the time scale of prediction is on the order of seconds. A Markov chain [12–14, 18] is effective for the prediction of this purpose. The third purpose is to generate more electricity. On this chapter, we focus on this third purpose.

There are two types of wind turbines. The major one has a horizontal axis, while the minor one has a vertical axis. The horizontal axis is more popular because it can attain better efficacy.

There are several factors one may control in a wind turbine with a horizontal axis. The examples include the direction of wind turbine (yaw angle), pitch angles, and speeds of rotations. Although mechanical details could be different, the problems for controlling these factors can be written mathematically in a similar way. As an example, we formulate a problem of yaw control.

In yaw control, the net benefits we can get are divided into two parts: the first part is benefits we may obtain; the second part is costs for controls. The unit of the net benefits is a currency: yen, US dollars, UK pounds, or other currencies. The benefits we may obtain from the energy production correlates with the amount of energy production. Thus, they are shown by using a power curve, a function $f(u)$ that returns the amount of energy produced given a wind speed u. Here the wind speed is perpendicular to the face of the rotor. Let v_t be the absolute wind speed at time t, θ_t, the wind direction, and $\varphi(t)$, the direction of the wind turbine. We also denote a set of v_t, θ_t, $\varphi(t)$ by v, θ and φ, respectively. Then, the benefits $b(\varphi, v, \theta)$ from time k to $k+K$ can be written as

$$\sum_{t=k+1}^{k+K} f(v_t \cos(\theta_t - \varphi(t))). \tag{2.1}$$

Since we have freedom for choosing the scale of the currency, we scale the currency in a way that the maximum electricity generated within 2 s yields a unit of the currency.

The costs for the yaw control include the electricity we need, replacements of devices due to stress, fatigue, and friction, and others coming from unknown sources. The term of the costs is a function of the orbit φ, wind speed v, and wind direction θ. Therefore, we denote it by $c(\varphi, v, \theta)$. In the simulations shown later, we assume that $c(\varphi, v, \theta)$ can be written as

$$\begin{aligned} &C_1 \sum_{t=k+1}^{k+K} |\varphi(t) - \varphi(t-1)| \\ &\quad + C_2 \sum_{t=k+1}^{k+K} |(\varphi(t) - \varphi(t-1)) - (\varphi(t-1) - \varphi(t-2))| \\ &\quad + C_3 \sum_{t=k+1}^{k+K} |\varphi(t) - \theta_t|. \end{aligned} \tag{2.2}$$

The first term depends on how much we turn a wind turbine. The second term depends on how much we change the angular velocity of wind turbine. The third term depends on the difference between the directions of the wind and the wind turbine.

The net benefits can be written as $b(\varphi, v, \theta) - c(\varphi, v, \theta)$. By replacing v_t and θ_t with their predictions $\hat{v}_t$ and $\hat{\theta}_t$, a problem of yaw control can be written as

$$\min_{\varphi} b(\varphi, \hat{v}, \hat{\theta}) - c(\varphi, \hat{v}, \hat{\theta}). \tag{2.3}$$

The above problem means that for yaw control, we need to predict the wind direction and absolute wind speed for the duration of K.

2.2 Characteristics for Time Series of the Wind

To predict the future wind, we need to know its properties. In this section, we discuss the characteristics of the wind.

2.2.1 Surrogate Data

To characterise the data sets, we used surrogate data analysis [21–25]. Surrogate data analysis is hypothesis testing. At the beginning of the analysis, one decides a null-hypothesis. Then we generate a set of random data that are consistent with the null-hypothesis. These random data are used for obtaining a confidence interval of a test statistic. If the value of the test statistic obtained from the original data is within the confidence interval, then one cannot reject the null-hypothesis. Otherwise, one rejects the null-hypothesis.

Common null-hypotheses are non-serial dependence [21], linearity [22, 25], and periodic orbits with uncorrelated noise [24]. In this chapter, we use the first two since the third surrogate has meaning when a time series is pseudo-periodic.

2.2.2 Results

In this section, we used a data set of the wind measured on 25 August 2004 at the top of a building in Institute of Industrial Science, The University of Tokyo. The measurement was of 50 Hz and it has three components, namely, the east wind, the north wind, and the upward wind. Part of data set is shown in Fig. 2.1.

First we preprocessed the data set. We divided a data set of the east and north winds into 36 segments of scalar time series of length 10,000. Then we matched the beginning and the end of time series [23] to avoid artefacts their mismatch may cause. By applying the method of Kennel [15] with four-dimensional embedding space with a uniform delay of 2 s, we confirmed the stationarity for 10 segments out of 36 segments. We used the delay of 2 s because this is a time scale we are interested in the later part of this chapter. We used the four-dimensional embedding space because in most cases we tested, the false nearest neighbour method [16] showed that with four-dimensional embedding space, the ratio of the false nearest neighbours is less

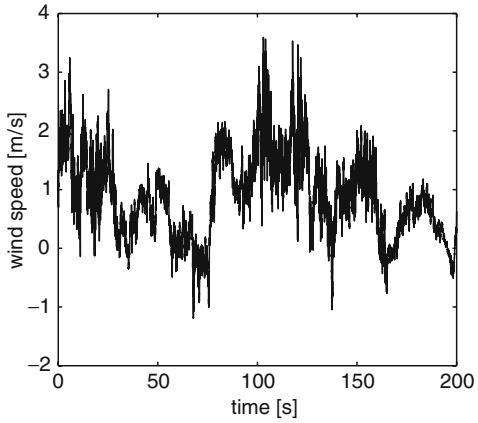

Fig. 2.1. Part of data set used in surrogate data analysis

than 1%. We had to exclude nonstationary segments since nonstationarity might cause a spurious rejection [26].

Second, we used random shuffle surrogates [21] for testing serial dependence. We used the Wayland statistic [27] for the test statistic. We used the embedding dimensions between 1 and 12. We generated 39 random shuffle surrogates and thus the significant level for each embedding dimension was 5%. To make the significant level of the multiple tests 1%, we need to have more than or equal to three rejections out of 12 embedding dimensions. We found that all the ten stationary segments have serial dependence. But a peculiar feature is that the Wayland statistic for the original data is greater than that for the random shuffle surrogates [5] (see Fig. 2.2). This may be interpreted

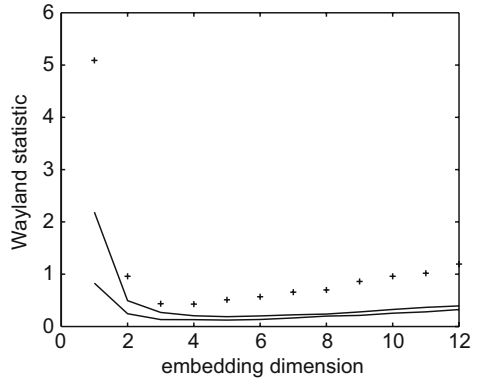

Fig. 2.2. Surrogate test for serial dependence. The *crosses* show the values obtained from the actual data set and the *solid lines*, the minimum and maximum for 39 random shuffle surrogates

that the original data are less deterministic than the random shuffle surrogates while this interpretation should be wrong. After testing some models, we found that this strange phenomenon could happen if an original data set is contaminated with either observational noise or dynamical noise [5]. The common characteristic between these two possible causes is that a time series has small fluctuations around trends. Thus, the wind may be considered as small fluctuations with long-term trends.

Third, we tested the nonlinearity. We generated iterative amplitude adjusted Fourier transform surrogates [22] and compared the original data sets and their surrogates with the Wayland statistic of the original data. We found a rejection in a multiple test for three segments out of 10 stationary segments. The number of rejections is significantly higher than the chance level. Thus the wind may be assumed to be a nonlinear process.

2.3 Modelling and Predicting the Wind

In the previous section, we discussed that a nonlinear model is appropriate for modelling the wind. In this section, we build a model and evaluate its performance by a prediction error.

2.3.1 Multivariate Embedding

In most cases, nonlinear time series analysis starts with delay embedding. Let $x_i(t)$ be the ith observable at time t. Let $x(t)$ represent whole the state at time t. Then, we choose

$$(x_i(t), x_i(t-\tau), x_i(t-2\tau), \cdots, x_i(t-(\kappa-1)\tau)). \tag{2.4}$$

If κ is sufficiently large, then this vector gives an embedding, meaning that the vector and $x(t)$ is one-to-one and the associated tangent space at each point is also one-to-one. For the comparison later, we call this vector uniform embedding.

In practice, Judd and Mees [10] extended the notion of delay embedding and defined the following vector:

$$(x_i(t-\tau_1), x_i(t-\tau_2), \cdots, x_i(t-\tau_\kappa)). \tag{2.5}$$

They call this vector non-uniform embedding. The method of Judd and Mees [10] fits a linear model and chooses the vector that minimises description length, an information criterion.

The non-uniform embedding was extended to multivariate time series by Garcia and Almeida [1]. Namely, one tries to construct a vector which looks like

$$(x_{i_1}(t-\tau_1), x_{i_2}(t-\tau_2), \ldots, x_{i_\kappa}(t-\tau_\kappa)). \tag{2.6}$$

Their method is based on the extension of false nearest neighbour method [16], a standard method for estimating the embedding dimension. In this chapter, we used the extension [8] of Judd and Mees [10], another method for obtaining an non-uniform embedding from a multivariate time series, since the method gives, within a shorter time, a non-uniform embedding which is as reasonable as the method of Garcia and Almeida.

2.3.2 Radial Basis Functions

The model we built was a radial basis function model since it can approximate any continuous function relatively well. We use $x^i(t)$ for showing a reconstruction for the ith coordinate at time t. Then a radial basis function model can be written as

$$x_i(t+1) = \delta_i + \alpha_i \cdot x^i(t) + \sum_l \beta_{i,l} \exp\left[-\frac{\|x^i(t) - \gamma_{i,l}\|^2}{2\nu^2}\right], \tag{2.7}$$

where δ_i, α_i, $\beta_{i,l}$, $\gamma_{i,l}$, and ν are parameters for the model. The centres of the radial basis functions were chosen using the technique of chaperons [9]. In this technique, one chooses a set of points from observations and adds Gaussian noise to them, whose standard deviation is 30% of that of the data. We prepared 100 radial basis functions using this technique. We also set ν to the standard deviation of the time series.

Since we have already decided $\gamma_{i,k}$ and ν, now our model is a pseudo-linear model and the remaining parameters may be decided by the least squares solution. But a simple application of the least squares solution will face the problem of overfitting. To avoid overfitting, we decided the remaining parameters for the radial basis function model as prescribed by Judd and Mees [9] using the Normalised Maximum Likelihood [19] for a model selection criterion. To explain the details, first let us define the Normalised Maximum Likelihood.

First we need to define a set of basis functions. In this chapter, the set is made of the 100 radial basis functions and linear terms. Suppose that now we have a number P of basis functions $\{\zeta_j : j \in F\}$, where $F = \{1, 2, \ldots, P\}$ is the set of indices for all the basis functions. Let D be the biggest delay among $\{\tau_i\}$. The length of given time series is denoted by N. Define $\tilde{N} = N - D$. Let V be the $\tilde{N} \times P$ matrix whose (q, r) component is the value for the rth basis function at time q, i.e.,

$$V = \begin{pmatrix} \zeta_1(x^i(D)) & \zeta_2(x^i(D)) & \cdots & \zeta_P(x^i(D)) \\ \vdots & & & \vdots \\ \zeta_1(x^i(t)) & \zeta_2(x^i(t)) & \cdots & \zeta_P(x^i(t)) \\ \vdots & & & \vdots \\ \zeta_1(x^i(N-1)) & \zeta_2(x^i(N-1)) & \cdots & \zeta_P(x^i(N-1)) \end{pmatrix}. \tag{2.8}$$

Denote a set of indices for basis functions by B. Thus, it holds that $B \subset F$. Let us denote by V_B the matrix that is formed from the columns of V with indices in $B = \{j_1, \ldots, j_J\}$, i.e.,

$$V_B = \begin{pmatrix} \zeta_{j_1}(x^i(D)) & \zeta_{j_2}(x^i(D)) & \cdots & \zeta_{j_J}(x^i(D)) \\ \vdots & & & \vdots \\ \zeta_{j_1}(x^i(t)) & \zeta_{j_2}(x^i(t)) & \cdots & \zeta_{j_J}(x^i(t)) \\ \vdots & & & \vdots \\ \zeta_{j_1}(x^i(N-1)) & \zeta_{j_2}(x^i(N-1)) & \cdots & \zeta_{j_J}(x^i(N-1)) \end{pmatrix}. \tag{2.9}$$

Let us also define ξ as

$$\xi = (x_i(D+1), \ldots, x_i(t+1), \ldots, x_i(N))^{\mathrm{T}}. \tag{2.10}$$

Here 'T' shows the transposition of matrix.

Let λ_B be the least squares solution for $\xi \approx V_B \lambda_B$. Then the prediction error e_B can be written as $e_B = \xi - V_B \lambda_B$. When minimising the squared error $e_B^{\mathrm{T}} e_B$, we can find the solution by

$$\lambda_B = (V_B^{\mathrm{T}} V_B)^{-1} V_B^{\mathrm{T}} \xi. \tag{2.11}$$

Define R by

$$R = \frac{1}{\tilde{N}} (V_B \lambda_B)^{\mathrm{T}} V_B \lambda_B. \tag{2.12}$$

Then the Normalised Maximum Likelihood [19] for a set of p basis functions B is given by

$$\mathcal{L}(B) = \frac{\tilde{N} - p}{2} \ln \frac{e_B^{\mathrm{T}} e_B}{\tilde{N}} + \frac{p}{2} \ln R - \ln \Gamma \left(\frac{\tilde{N} - p}{2} \right) - \ln \Gamma \left(\frac{p}{2} \right) - \ln p. \tag{2.13}$$

Here Γ shows the Gamma function.

Using the Normalised Maximum Likelihood and these notations, we can write down the algorithm proposed in [9] for selecting an optimal set of basis functions in the following way:

1. Normalise V so that each column has unit length.
2. Let B and B' be empty sets.
3. Obtain the prediction error. If B' is empty, then $e_{B'} = \xi$. If not, then $e_{B'} = \xi - V_{B'} \lambda_{B'}$. Here $\lambda_{B'}$ can be obtained using the formula of (2.11).
4. Find the basis function that matches the prediction error best. Let $\mu = V^{\mathrm{T}} e_{B'}$. Then the biggest component of μ corresponds to the best basis function matching to the prediction error. Let g be the index for the best matching basis function. Let $B' \leftarrow B' \cup \{g\}$.
5. Find the basis function in B' that least contributes to making the error small. Let h be the index for the basis function whose corresponding $\lambda_{B'}$ is the smallest. If $g \neq h$, then $B' \leftarrow B' \backslash \{h\}$ and go to Step 3.

6. If B is empty or $\mathcal{L}(B') < \mathcal{L}(B)$, then set $B \leftarrow B'$ and go back to Step 3.
7. The chosen B is the optimal set of basis functions.

We used the above algorithm for deciding δ_i, α_i, and $\beta_{i,l}$. Namely, for basis functions which are not selected, we set the corresponding components to 0. For selected basis functions, we use values obtained from the above fitting.

2.3.3 Possible Coordinate Systems

There are two possible coordinate systems for representing a wind vector. The first one is the polar coordinate system. The second one is the rectangular coordinate system. The problem of the polar coordinate system is how to represent the wind direction. The wind direction has a value between 0° and 360°, which is on a ring. If one tries to show the wind direction using a value in an interval, then one has to split the ring somewhere and it causes discontinuity. As a result, the wind direction cannot be predicted well [6]. Thus, the rectangular coordinate system is better than the polar coordinate system for predicting the wind direction.

2.3.4 Direct vs. Iterative Methods

The model now at our hands predicts a step ahead. However, as discussed in Sect. 2.1, we need to predict the wind direction and absolute wind speed for a certain range of time. There are two options for it: The first option is to prepare several models each of which has a different prediction step. This approach is called a direct method. The second option is to use a model for predicting a step ahead several times and realise a multiple step prediction. This approach is called an iterative method.

There are some discussions on which model is better on a certain occasion [11, 17]. Generally speaking, when we have a good one-step prediction, then an iterative method is better. Otherwise, a direct method might be better. Judd and Small [11] proposed a mixture of direct and iterative methods. In their method, one first uses an iterative method and predicts the future values. This step is called ϕ-step since the one-step model is shown using ϕ. Then one uses a corrector ψ that makes the prediction more accurate. This step is called ψ-step due to the notation of the corrector. As a total, the method is called the $\psi\phi$ method.

2.3.5 Measurements of the Wind

The data sets we used were measured at about 1 m high on the campus of the Institute of Industrial Science, The University of Tokyo. We used two identical anemometers which record the east, the north, and the upward winds with 50 Hz. We measured the wind for nine different days between September 2005 and May 2006. On some days, we placed the two anemometers 5 m apart in

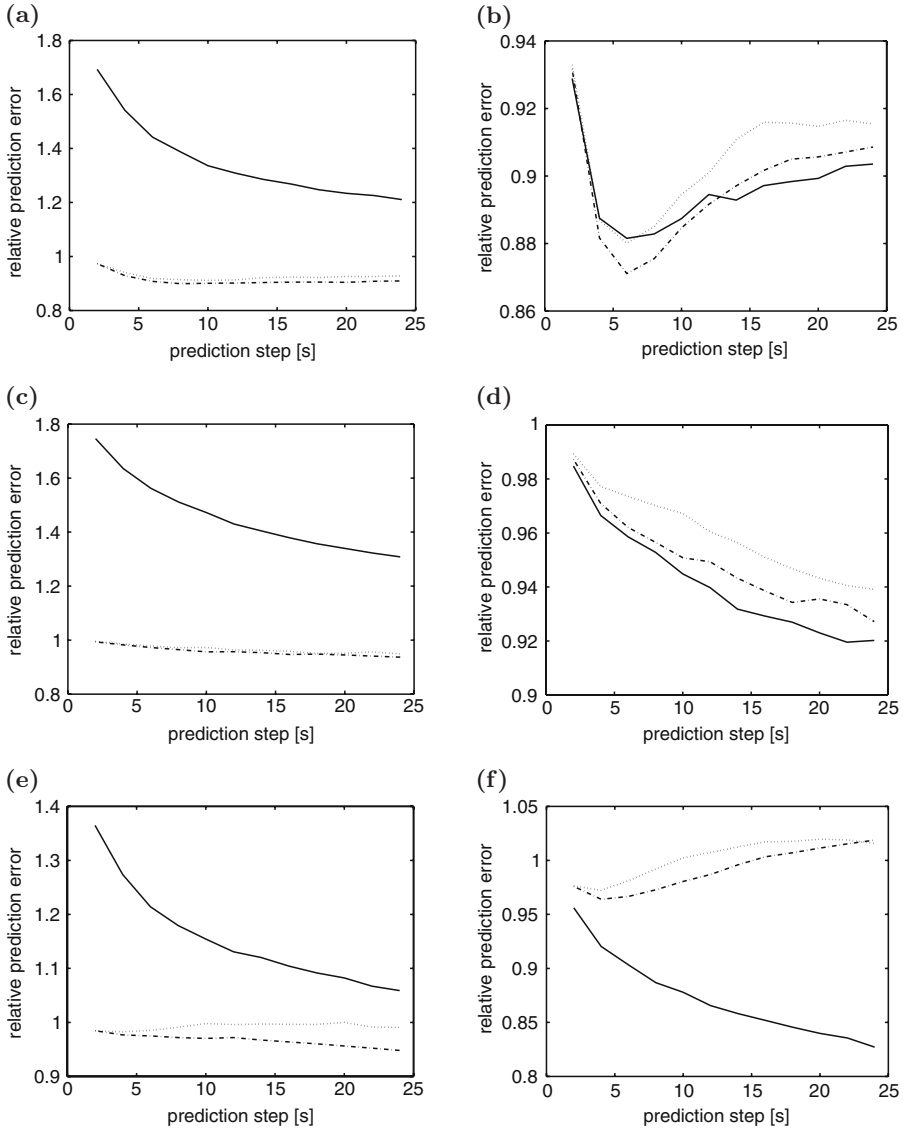

Fig. 2.3. Means of root mean square errors for the compared combinations of methods relative to those of persistent prediction. (**a**) and (**b**) are cases where the additional observation was at upstream. (**c**) and (**d**) are cases where the additional observation was at downstream. (**e**) and (**f**) are cases where the additional observation was nearby but at neither downstream nor upstream. (**a**), (**c**), and (**e**) show root mean square errors for the wind direction, and (**b**), (**d**), and (**f**), those for the absolute wind speed. In each part, the *solid line* shows the case of polar coordinates with the direct method, the *dotted line*, that of rectangular coordinates with the direct method, and the *broken line*, that of rectangular coordinates with the $\psi\phi$ method

the north–south direction. On the other days, we placed them 5 m apart in the east–west direction. Since we are interested in the dynamics of 2 s order, we took the moving average of 2 s and resampled it by 2 s.

We used measurements taken from the two points for predicting the wind at one of them as we can expect better prediction by doing this [7].

2.3.6 Results

In the previous sections, we argued that there are two coordinate systems and two possible methods for the prediction. Thus, theoretically there are four possible combinations. In this section, however, we compare three of them, namely, the polar coordinates with the direct method, the rectangular coordinates with the direct method, and the rectangular coordinates with the $\psi\phi$ method, since the polar coordinates with an iterative method does not provide good prediction since they have to use the prediction of the wind direction several times.

In Fig. 2.3, we compared the performances of the three combinations of the methods by the prediction error for each method relative to that for the persistent prediction, where we used the value of 2 s before as a prediction.

When we predicted the wind direction, the rectangular coordinates with the $\psi\phi$ method achieved smaller mean prediction errors than the other two combinations (Fig. 2.3a, c, e). We interpret this results as follows: Because the wind direction takes a value on the ring, the polar coordinates are not a good idea for representing the wind direction. By using the $\psi\phi$ method, we can make the prediction errors smaller compared to the direct prediction.

When we predicted the absolute wind speed (Fig. 2.3b, d, f), the polar coordinates with the direct method gave the smallest mean prediction error for all cases except for short prediction steps of the case where the additional observation was at upstream. We think that the polar coordinates were better

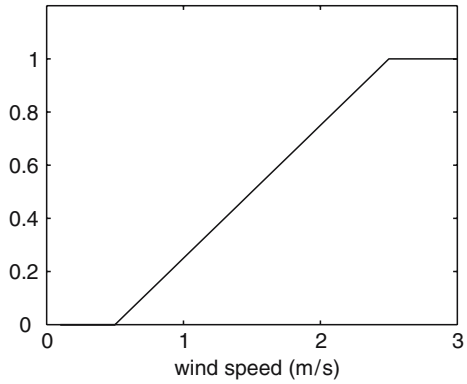

Fig. 2.4. Power curve used for the simulation

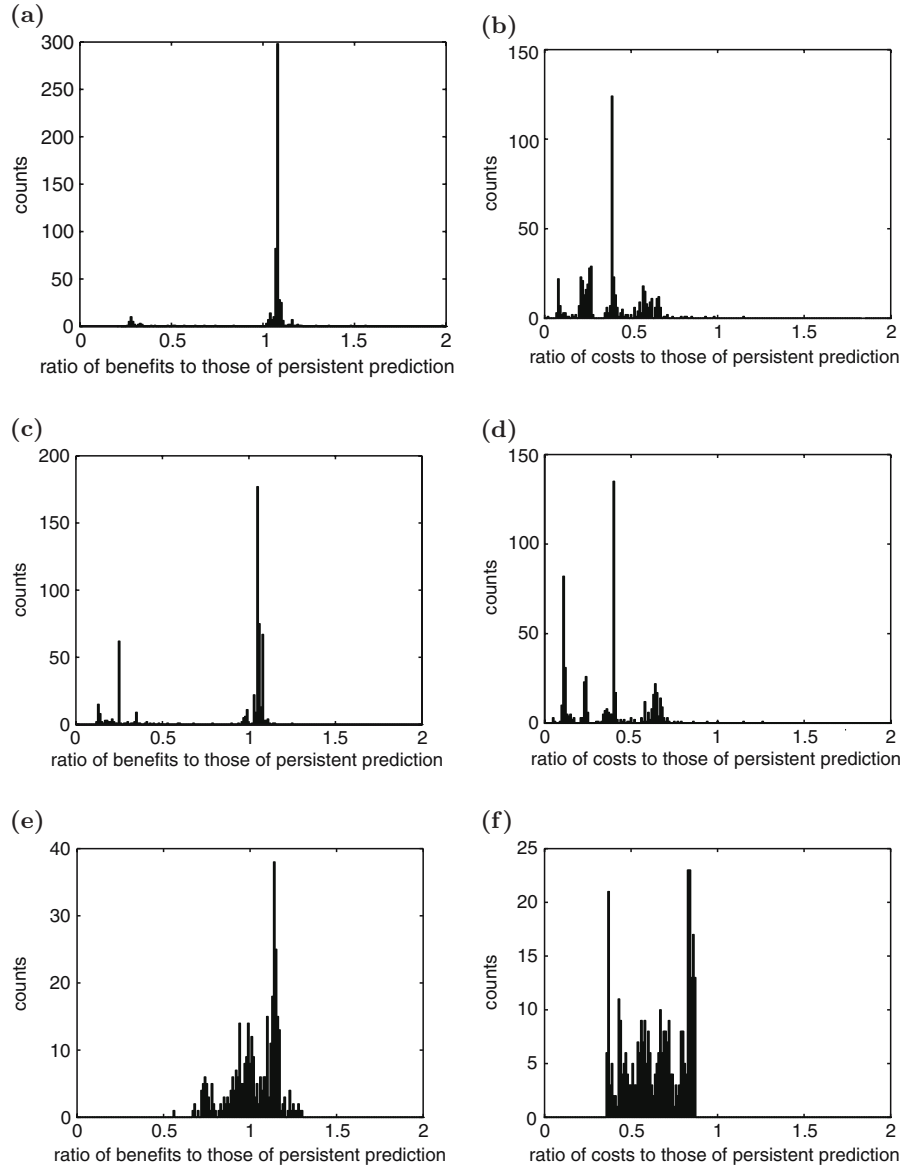

Fig. 2.5. Results of simulations for energy production. (**a**), (**c**), and (**e**) show the histograms of ratios of expected net benefits for the combination of the proposed prediction methods to those for the persistent prediction. (**b**), (**d**), and (**f**) show the histograms of ratios of expected costs for controlling a wind turbine based on the proposed prediction to those based on the persistent prediction. (**a**) and (**b**) are cases where the additional observation was at upstream. (**c**) and (**d**) are cases where the additional observation was at downstream. (**e**) and (**f**) are cases where the additional observation was nearby but at neither downstream nor upstream

for predicting the absolute wind speed because the polar coordinates represent what we want to predict directly.

2.4 Applying the Wind Prediction to the Yaw Control

In Sect. 2.3, we observed that the wind direction was predicted well when the rectangular coordinates with the $\psi\phi$ method was used, while the absolute wind speed was predicted well when the polar coordinates and the direct method were used. In this section, we compared the combination of these methods with the persistent prediction in expected energy.

From the actual data, we predicted the wind directions and absolute wind speeds for prediction steps between 2 and 24 s. Then we fed the predictions to the model of wind turbine presented in Sect. 2.1 and decided the control policy. For estimating energy production, we used the actual wind data.

We used a power curve shown in Fig. 2.4 for the simulation. We set $C_1 = C_2 = C_3 = 0.01$.

We used the polar coordinates with the direct method and the rectangular coordinates with the $\psi\phi$ method for predicting the absolute wind speed and the wind direction, respectively. This combination is the best, based on the results of Sect. 2.3. We compared the results with the case where we used the persistent prediction for both the absolute wind speed and the wind direction.

The results were shown in Fig. 2.5. The median of ratio of the expected net benefits for the proposed prediction to those for the persistent prediction is greater than 1. The median of ratio of the expected control costs for the proposed prediction to those for the persistent prediction is smaller than 1. These results mean that the proposed prediction works well for controlling a wind turbine. The above observations were always true and do not depend on the place of the additional observation point much.

2.5 Conclusions

In this chapter, we showed it is possible that wind modelling may help to increase energy production. To show this, we first formulated the problem for controlling the yaw angle of a wind turbine and found that we need to predict the wind direction and the absolute wind speed for a certain range of the future. Next, we investigated the properties of time series of the wind using surrogate data analysis. We showed that the time series always have serial dependence and they sometimes have nonlinearity. We also argued that times series of the wind may be characterised by small fluctuations with trends. These findings are positive signs for the prediction. Then, we modelled the wind and found that the wind direction is predicted well by the rectangular coordinates and the $\psi\phi$ method, and the absolute wind speed is predicted well if one uses the polar coordinates and the direct method. Finally, we applied

the prediction of the wind to the simulation of wind turbine control. We found that the nonlinear prediction can potentially increase the energy production. An important point is that although our gain of information is small in terms of the root mean square error, it is big enough for controlling a wind turbine optimally.

We feel that the methods discussed here could be useful for controlling a small wind turbine since a small wind turbine can be directed with a small force very quickly, and in the scale of a small wind turbine, the wind at the edges of the blades is not so much different from that at the centre.

The focus of this chapter has been that a heterogeneous data fusion strategy is useful for controlling a wind turbine, and therefore the models of turbine, stress, fatigue, and friction used are synthetic. Although these models are not guaranteed to provide a feasible and safe solution for a real wind turbine, we believe that they are sufficiently realistic to illustrate the proposed framework.

Acknowledgement

This study was partially supported by the Industrial Technology Research Grant Program in 2003, from the New Energy and Industrial Technology Development Organization (NEDO) of Japan.

References

1. Garcia, S.P., Almeida, J.S.: Multivariate phase space reconstruction by nearest neighbor embedding with different time delays. Physical Review E **72**(2), 027205 (2005)
2. Goh, S.L., Chen, M., Popvic, H., Aihara, K., Obradovic, D., Mandic, D.P.: Complex-valued forecasting of wind profile. Renewable Energy **31**(11), 1733–1750 (2006)
3. Goh, S.L., Mandic, D.P.: A complex-valued RTRL algorithm for recurrent neural networks. Neural Computation **16**(12), 2699–2713 (2004)
4. Goh, S.L., Mandic, D.P.: Nonlinear adaptive prediction of complex-valued signals by complex-valued PRNN. IEEE Transactions on Signal Processing **53**(5), 1827–1836 (2005)
5. Hirata, Y., Horai, S., Suzuki, H., Aihara, K.: Testing serial dependence by Random-shuffle surrogates and the wayland method. Physics Letters A (2007). DOI 10.1016/j.physleta.2007.05.061
6. Hirata, Y., Mandic, D.P., Suzuki, H., Aihara, K.: Wind direction modelling using multiple observation points. Philosophical Transacations of the Royal Society A (2007). DOI 10.1098/rsta.2007.2112
7. Hirata, Y., Suzuki, H., Aihara, K.: Predicting the wind using spatial correlation. In: Proceedings of 2005 International Symposium on Nonlinear Theory and its Applications (NOLTA 2005) (2005)

8. Hirata, Y., Suzuki, H., Aihara, K.: Reconstructing state spaces from multivariate data using variable delays. Physical Review E **74**(2), 026202 (2006)
9. Judd, K., Mees, A.: On selecting models for nonlinear time-series. Physica D **82**(4), 426–444 (1995)
10. Judd, K., Mees, A.: Embedding as a modeling problem. Physica D **120**(3–4), 273–286 (1998)
11. Judd, K., Small, M.: Towards long-term prediction. Physica D **136**(1–2), 31–44 (2000)
12. Kantz, H., Holstein, D., Ragwitz, M., Vitanov, N.K.: Extreme events in surface wind: Predicting turbulent gusts. In: S. Bocaletti, B.J. Gluckman, J. Kurths, L.M. Pecora, R. Meucci, O. Yordanov (eds.) Proceedings of the 8th Experimental Chaos Conference, no. 742 in AIP Conference Proceedings. American Institute of Physics, New York (2004)
13. Kantz, H., Holstein, D., Ragwitz, M., Vitanov, N.K.: Markov chain model for turbulent wind speed data. Physica A **342**(1–2), 315–321 (2004)
14. Kantz, H., Holstein, D., Ragwitz, M., Vitanov, N.K.: Short time prediction of wind speeds from local measurements. In: J. Peinke, P. Schaumann, S. Barth (eds.) Wind Energy: Proceedings of the EUROMECH Colloquium. Springer, Berlin Heidelberg New York (2006)
15. Kennel, M.B.: Statistical test for dynamical nonstationarity in observed time-series data. Physical Review E **56**(1), 316–321 (1997)
16. Kennel, M.B., Brown, R., Abarbanel, H.D.I.: Determining embedding dimension for phase-space reconstruction using a geometrical construction. Physical Review A **45**(6), 3403–3411 (1992)
17. McNames, J.: A nearest trajectory strategy for time series prediction. In: Proceedings of the International Workshop on Advanced Black-Box Techniques for Nonlinear Modeling (1998)
18. Ragwitz, M., Kantz, H.: Detecting non-linear structure and predicting turbulent gusts in surface wind velocities. Europhysics Letters **51**(6), 595–601 (2000)
19. Rissanen, J.: MDL denoising. IEEE Transactions on Information Theory **46**(7), 2537–2543 (2000)
20. Roulston, M.S., Kaplan, D.T., Hardenberg, J., Smith, L.A.: Using medium-range weather forecasts to improve the value of wind energy production. Renewable Energy **28**(4), 585–602 (2003)
21. Scheinkman, J.A., LeBaron, B.: Nonlinear dynamics and stock returns. Journal of Business **62**(3), 311–337 (1989)
22. Schreiber, T., Schmitz, A.: Improved surrogate data for nonlinearity tests. Physical Review Letters **77**(4), 635–638 (1996)
23. Schreiber, T., Schmitz, A.: Surrogate time series. Physica D **142**(3–4), 346–382 (2000)
24. Small, M., Yu, D., Harrison, R.G.: Surrogate test for pseudoperiodic time series. Physical Review Letters **87**(18), 188101 (2001)
25. Theiler, J., Eubank, S., Longtin, A., Galdrikian, B., Farmer, J.D.: Testing for nonlinearity in time-series: the method of surrogate data. Physica D **58**(1–4), 77–94 (1992)
26. Timmer, J.: Power of surrogate data testing with respect to nonstationarity. Physical Review E **58**(4), 5153–5156 (1998)
27. Wayland, R., Bromley, D., Pickett, D., Passamante, A.: Recognizing determinism in a time-series. Physical Review Letters **70**(5), 580–582 (1993)

http://www.springer.com/978-0-387-74366-0

Signal Processing Techniques for Knowledge Extraction and Information Fusion

Mandic, D.; Golz, M.; Kuh, A.; Obradovic, D.; Tanaka, T. (Eds.)

2008, XXII, 320 p., Hardcover
ISBN: 978-0-387-74366-0